Difference in genetic architecture is a key driver in plant-to-plant interaction: case study of height and rust damages in Populus nigra

Authors: Mathieu Tiret[1,3*], Leopoldo Sánchez[2], Martin Lascoux[1].

Affiliations:

- 1: Program in Plant Ecology and Evolution, Department of Ecology and Genetics, EBC and SciLife Lab, Uppsala University, Uppsala, Sweden
- 2: BioForA, INRAE, ONF, Orléans, France.
- 3: IGEPP, INRAE, Institut Agro, Université de Rennes, Domaine de la Motte, Le Rheu, France.

* corresponding author: mathieu.tiret@inrae.fr

Abstract: (179 words)

Main text: 5,100 words.

keywords: group selection, genomic selection, Populus nigra, quantitative genetics.

Abstract:

Adaptation to competition during the evolutionary history of plants leads to a reduction of the overall group performance of plant elite material in the field. Traits related to competitive ability can be affected by the presence or absence of kin in the neighborhood. Consequently, local relatedness might reveal plant-to-plant interaction that can enhance the predictive abilities of genomic models when accounted for. However, recurrent family selection increases relatedness among all elite material and can blur the effect of relatedness on neighbors' phenotypes. To overcome this difficulty, we analyzed data from the French breeding program of *Populus nigra* L., where 1,452 genotypes were replicated six to eight times, each time encountering a different neighborhood. We assessed local relatedness and investigated genomic estimated breeding values on tree height and rust vulnerability with a single-step GBLUP incorporating local relatedness as a covariate. Results suggests that including local relatedness as an additional factor to GBLUP models is significantly more important for rust resistance than for tree height, mainly due to their contrasting genetic architecture – oligogenic for the former and polygenic for the latter.

Introduction

Breeding generally consists in redirecting evolutionary trade-offs towards new equilibria that often decrease fitness in favor of other economically interesting traits, or towards paths that were insufficiently explored by evolution in natural populations, such as group selection (Weiner, 2019). Although the importance of group selection in nature is controversial (Maynard Smith, 1964; Lewontin, 1970; Wilson & Wilson, 2007; Okasha, 2020), in a breeding program, group selection can be used to improve overall performance (e.g., robust productivity, tolerance to biotic or abiotic stress, or long-term response to selection), by keeping only those candidates that contribute favourably to plant-to-plant interactions. The performance of an individual can then be decomposed into direct and indirect breeding values (also called direct and indirect genetic effects), where the former is the intrinsic value of an individual without any competitors, and the latter the ability of the individual to increase or decrease performance due to competition (Griffing, 1967; Bijma & Wade, 2008). Breeding can benefit from accounting for both, especially in contexts in which the indirect genetic effect is strong, such as when intraspecific competition is strong among candidates (Weiner et al., 2017). Indeed, selfish strategies (in the sense of selfish genes), although increasing individual fitness, are often costly for the populations in breeding schemes - and breeding circumventing such strategies ended up with very successful results (e.g., Donald, 1981; Donald and Hamblin, 1983; Weiner et al., 2010). Competitive behavior can, therefore, be a burden that breeders might want to select against. Despite the early success of some ideotypes optimizing group performance, current breeding programs do not necessarily focus on integrating this dimension (e.g., Denison et al., 2003; Murphy et al., 2017; Montazeaud et al., 2020). Consequently, the pool of elite genotypes used nowadays might be mostly composed of selfish genotypes, since early mass selection, bypassing group dynamic, favored selfish genotypes for their vigorous phenotypes (Murphy et al., 2017). It is

therefore increasingly important in order to reach sustained genetic gain in breeding programs to counteract the effect of natural selection acting at the deployment phase, and to correct past artificial selection trajectories focussed on competitive (i.e., selfish) individuals .

In the specific case of plant breeding, resource competition between candidates occurs with the nearest plants (Casper et al., 1997; Milbau et al., 2007; File et al., 2011). The intensity of competition among neighbors may depend on their relatedness, or local relatedness, either because of kin selection, which predicts that relatives may cooperate (Hamilton, 1964), or niche partitioning, which predicts, on the contrary, that similar individuals may compete for similar resources (Silvertown, 2004). Therefore, plant-to-plant interaction can partly be due to local relatedness in one way or the other (Cahill et al., 2011), so that classic models can be improved by incorporating the information of neighboring genotypes. Although kin recognition was reported to be not particularly relevant in crop species because of their already high relatedness (e.g., Murphy et al., 2017), we might be able to detect it nonetheless in breeding schemes that have been less intensive, such as forest tree breeding. Group selection is in fact expected to give better genetic progress for perennial species, since (i) inbreeding coefficient is much lower than in crop species (even though inbreeding depression can be higher; Lesaffre & Billiard, 2021), and (ii) positive or negative interactions between neighbors last a lifetime.

Part of the phenotypic variance is due to the micro-environmental heterogeneity, and accounting for it has been shown to improve predictions (Cappa et al., 2022). Among the micro scale heterogeneity, local relatedness by variable neighborhood can create heterogeneity, hence a phenotypic variance that, when not accounted for, can bias genetic estimates. To account for heterogeneity caused by local relatedness, we chose to conduct our analyses on *Populus nigra* L.. Black poplar is a Eurasian riparian forest tree that contributes, as a parent along with *Populus deltoides* Bartr. ex Marsh., to one of the most widely used hybrid tree in forest breeding (*Populus x canadensis*), and is widely deployed as

clones, constituting a model in which kin recognition, if any, should be the strongest. The dataset, stemming from the French breeding program with 1,452 genotypes replicated six to eight times, created different neighborhoods for each replicated genotype (Pégard et al., 2020), all resulting from controlled crosses of 34 parents from natural populations, some of which were already used in the breeding programme for their performance. To detect any signal of group selection, we focused on two quantitative traits relevant for breeding, tree height and rust vulnerability. Growth of Black poplar is particularly susceptible to foliar rust, caused by a fungus (*Melampsora larici-populina* Kleb.) that leads to a reduction in photosynthesis efficiency, and might lead to the death of susceptible clones (Legionnet et al., 1999). Rust development is strongly influenced by susceptibility of nearby trees, hence putatively linked to local relatedness, whereas tree height is a poor indicator of competition and is mostly related to the fertility of the trial. Height is known to have a polygenic architecture (Du et al., 2016), and rust resistance to have a mono- or oligogenic architecture (e.g., Jorge et al., 2005), implying that relatedness – as the amount of shared alleles – will have different consequences on those two traits: genetic redundancy of height probably making it less sensitive to local relatedness than rust resistance.

In order to assess the contribution of local relatedness in the context of genomic selection (Meuwissen et al., 2001), we performed genomic evaluations with a multitrait single-step Genomic Best Linear Unbiased Predictor (ssGBLUP; Legarra et al., 2009; Christensen et al., 2010). Estimating breeding values with ssGBLUP is a solid baseline in forest trees as recently shown (e.g., Cappa et al., 2019; Ratcliffe et al., 2017), especially its multitrait version that is known to give higher accuracy (Calus et al., 2011). By including local relatedness and spatial micro-environmental autocorrelation as random effects in ssGBLUP models, we assessed whether plant-to-plant interactions – phenotypic covariance between neighbors – could be due to local relatedness. We assessed local relatedness with different subsets of SNPs, each maximizing or minimizing one of the following features: Minor Allele Frequency, Ancestry Informativeness Coefficient, significance in a Genome Wide

Association Study, or heritability. We show that local relatedness significantly impacts the phenotype of an individual and, when surrounded by related individuals, rust damage is significantly more important, whereas no interaction was visible on tree height. Differences in genetic architecture seem to play a role in plant-to-plant interactions.

6

Material and Methods

Plant material. The study is based on previously published data (Pégard et al., 2019, 2020). Seventeen male and 17 female *Populus nigra* were sampled in France, from 21 natural populations with no a priori selection and 13 from the French poplar breeding program for their performance on a range of traits, including growth and rust resistance. These individuals were used as parents in a factorial crossing plan and double-pair mating scheme. Clones of both parents and progeny, and a hundred additional individuals from breeding programs, were grown in four sequential experimental trials (parallel strips of two lines of trees, with an inter-strip spacing of 1m and an inter-strip spacing of 2 metres) at the same location (Guéméné-Penfao, France, 47°37’59”N, 1°49’59”W), each with a randomized incomplete 26 block design of single tree-plots (0.9 m x 1.0 m). In total, the experiment comprised 10,301 trees (including 7,169 trees with genotype information), 42 full-sib families, 5 half-sib families, 1,452 genotypes (each replicated on average 7.09 times), and an Unknown Parent Group (UPG) of 105 genotypes (Table S1). Family size ranged from 1 to 119, with an average of 30.2 genotypes per family. Twenty genotypes and 17 families were shared across the four trials.

Phenotype measurements. We focused on two phenotypic traits on one-year-old trees: height and rust vulnerability (both measured on field). Height was assessed with a graduation rod (in cm), and rust vulnerability (natural infection) was assessed on a scale of 1 to 9 : 1 when no rust was observed on the tree and 9 when more than 75% of lamina was covered by rust on more than 25% of the leaves (Legionnet et al., 1999). The homogeneity of rust pressure across the trial was assured by the level of infection measured on control individuals, being equally infected across blocks (clone ID: BDG). Some missing values were present across the trials (dead trees or unexploitable data), but at least 95.29%, 96.05%,

7

and 95.13% of the trees were phenotyped for height, rust vulnerability, or both traits, respectively. Given the low missing rate, we assumed that missing values only marginally unbalanced the block design, and so we used default parameters of the software packages for handling missing values when analyzing the data.

In each trial, every phenotype was first corrected for micro-environmental heterogeneity with a multitrait mixed model as follows:

$$Y_{ijkl} = \mu + BLOCK_i + SPLINE + e_{ijkl}$$

where 'Y_{ijkl}' is the l-th phenotype of the k-th replicate of the j-th genotype in the i-th trial, μ is the grand mean, '$BLOCK_i$' the random effect of the i-th block, '$SPLINE_i$' B-spline spatial autocorrelation correction over the surface of rows and columns (Cappa & Cantet, 2007), and 'e_{ijkl}' the residuals. Both the block effect and the residuals follow a Gaussian distribution with diagonal covariance matrices, and the model was fitted separately by trial. We used the function *remlf90* (R package *breedR*; Munoz and Sanchez, 2014) with the parameters 'model' set to 'splines' and 'method' set to 'em'. All further analyses were performed on the residuals of this model, i.e., on spatially adjusted phenotypes.

Genomic data. Out of the 1,452 genotypes, 1,034 were genotyped (25 parents and 1,009 offspring), using a *Populus nigra* 12K custom Infinium Bead-Chip (Illumina, San Diego, CA) (Faivre-Rampant et al., 2016). Details of the DNA extraction protocol, bioinformatic pipelines, and SNP mapping on the 19 chromosomes are given in Faivre-Rampant et al. (2016) and Pégard et al. (2019, 2020). It is worth noting that the SNP chip array included SNP in QTLs and expression candidate genes associated with, among other traits, rust resistance, but not with vertical growth. We retained SNPs with a Minor Allele Frequency (MAF) > 5%; in total, 7,129 SNPs were retained for further analyses (out of 7,513 initial SNPs).

8

Genomic relationship matrix. In order to build the relationship matrix necessary for inferring breeding values, we combined pedigree and genomic information (Legarra et al., 2009; Christensen et al., 2010). The pedigree relationship matrix A^{Γ} (following the notation of Legarra et al., 2009) was built using the tabular rule method (Emik and Terrill, 1949), modified to account for a single metafounder (assuming a single base population for the Unkown Parent Group or UPG; Legarra et al., 2015), with a self-relationship of $\gamma = 8\sigma_p^2$, with σ_p^2 the variance of allele frequencies across markers (Garcia-Baccino et al., 2017). The combined relationship matrix H was summarized in Aguilar et al. (2019), and is:

$$H^{-1} = (A^{\Gamma})^{-1} + (0,0;0;\ G^{-1} - (A_{22}^{\Gamma})^{-1}) \qquad (1),$$

where A_{22}^{Γ} is the submatrix of A^{Γ} corresponding to the genotyped individuals, $G = (1-\alpha)\ (\omega_a + \omega_b \times G_V) + \alpha\ A_{22}^{\Gamma}$, with G_V the genomic relationship matrix estimated from the SNPs and scaled following the first scaling method of Van Raden (2008), α a scaling parameter (here equal to 0.05), and ω_a and ω_b chosen to equate the average inbreeding and the average relationships in G_V and A_{22}^{Γ} as in Christensen et al. (2012). As the sample size was relatively small, the matrix H^{-1} was obtained by simply inverting H with the function *solve* (R package *base*).

Population structure. In order to control for population structure and avoid spurious associations, we computed a distance matrix 1 − H*, where H* is the correlation matrix obtained from H using the function *cov2cor* (R package *stats*), and the minus sign is to convert similarities to distances. We then used Multidimensional Scaling (MDS) on the distance matrix with the function *cmdscale_lanczos* (R package *refund*; Goldsmith et al., 2022; Miller, 2022) with the parameter 'k' set to 5 (hence explaining > 90% of the variance), and 'eig' set to 'TRUE'. Negative eigenvalues were set to null, and the variance explained by an axis was computed as the ratio between its squared eigenvalue and the sum of the squared eigenvalues. Additionally, to assess how well the family structure was captured, we

measured the variable V_F defined as the average within family variance on the first five axes (the lower the V_F, the better the family structure is captured). To make MDSs comparable, we normalized V_F by the sum of squares of the first five eigenvalues.

Breeding value inferences. The spatially adjusted phenotypes were then used to infer the breeding values with a multitrait single-step Genomic Best Linear Unbiased Predictor (ssGBLUP), as follows:

$$Y_{ijkl} = \mu + mds1_j + mds2_j + TRIAL_i + ANIMAL_j + e_{ijkl} \quad , \qquad (2)$$

where 'Y_{ijkl}' is the l-th phenotype of the k-th replicate of the j-th genotype in the i-th trial, μ is the grand mean, '$mds1_j$' and '$mds2_j$' the fixed effects on the j-th genotype of the first and second axes of the MDS, respectively, '$TRIAL_i$' the random effect of the i-th trial, '$ANIMAL_j$' the polygenic effect of the j-th genotype, and 'e_{ijkl}' the residuals. Both the trial effect and the residuals follow a Gaussian distribution with diagonal covariance matrices, and the polygenic effect follows a Gaussian distribution with a covariance matrix equal to k.H x Σ, where k is a scaling parameter equal to 1 - γ/2 (Legarra et al., 2015), H the combined relationship matrix, x the Kronecker product, and Σ the 2x2 covariance matrix between height and rust vulnerability. Estimates of coefficients and variance components of model (2) were obtained with the function *remlf90* (R package *breedR*) through one run with the 'method' parameter set to 'em' until convergence, then another run with the parameter 'method' set to 'ai' and the parameter 'progsf90.option' set to 'maxrounds 1'. The output estimate of '$ANIMAL_j$' is the Estimated Breeding Value (EBV) of the j-th genotype. The additive variance was obtained from the diagonal elements of Σ, and used to estimate heritability (the denominator of which also comprises the residual variance). The predictive ability (PA) of the model was defined as Pearson's correlation coefficient between the breeding values re-estimated from the effect sizes (see below) and the adjusted phenotypes corrected by the trial effect (i.e., $Y_{ijkl} - TRIAL_i$).

Genome-Wide Association Study (GWAS). Following the equations of Aguilar et al. (2019), the effect size of the SNPs was back-solved from the EBVs, along with their standard error and their p-values. This process was performed trait by trait (i.e., without accounting for the multitrait dimension) without loss of information, and taking all effects as fixed, as the Pearson's correlation between the ssGBLUP's EBV and the breeding values re-estimated by the effect sizes was greater than 0.999.

With the estimated effect sizes and the standard errors, we also computed an alternative to the p-value accounting for multiple testing: the local false sign rate (lfsr) estimated with an empirical Bayes approach for adaptive shrinkage using the function *ash* (R package *ashr*; Stephens, 2017). In order to detect GWAS peaks (regions in the chromosomes with a high density of significant SNPs), we used a custom peak detection script on the profile of lfsr (Tiret & Milesi, 2021) with default parameters. The script filtered out significant hits that are not statistically detected as a peak which is defined here as an abnormally high concentration of significant SNPs in a small chromosomic area.

Neighborhood. In order to account for the effect of the neighborhood, we estimated the breeding values with an additional fixed effect, the local relatedness, defined as the average relationship (from the matrix H) between a focal individual and its neighbors (eight or less if on boundaries; as the king's moves on a chessboard). Local relatedness was orthogonal to any micro-environmental effect, because of the random block design. The re-estimated breeding values were denoted nEBV.

SNP subsets. We investigated the effect of sampling SNPs on the ssGBLUP (i.e., weighted ssGBLUP). We selected subsets based on population and quantitative genetics features computed after a first run of ssGBLUP: MAF, Ancestry Informativeness Coefficient (AIM; Rozenberg et al., 2003), and for each trait, significance in the GWAS, and additive variance.

For each feature, we kept one-tenth of the whole set (713 SNPs, a sample size close to previous studies on weighted GBLUP, e.g., Li et al., 2018) with either the smallest or the largest values, ending up with 12 subsets. AIM was estimated per family with the R script provided by Cappa et al. (2022). Additive variance explained by a SNP was estimated as $2p(1-p)a^2$, where p is the MAF, and a the effect size (assuming no dominance nor interaction deviation of the genetic variance; p.129, Falconer, 1989). We re-estimated the combined relationship matrix for each SNP subset by re-estimating in the equation (1) the genomic relationship matrix G_V with the SNP subset. With the re-estimated matrices H, we re-performed the MDSs, and re-estimated the PAs of the EBVs and nEBVs (where local relatedness were measured with the re-estimated H).

Statistical tests. For each SNP subset, we computed the confidence interval of the Predictive Ability (PA) with a 1000 iteration bootstrap (re-sampling individuals), without re-estimating the covariance matrix Σ. Here, the bootstrap was only used to assess the variance, so that we centered the bootstrapped PA around the true PA. To assess the effect of sampling, these subsets were compared to 1000 random samples of 713 SNPs (the size of the SNP subsets). Comparisons were performed with a Student's one-sample *t*-test (denoted t_1 with a degree of freedom or df of 999 corresponding to the number of bootstrap iterations), or a Welch two-sample *t*-test (denoted t_2 with a varying df), both using the function *t.test* (R package *stats*). The sign of the *t* statistic is arbitrarily reported as positive when greater than a baseline (e.g., the true PA), and negative when not. Models were compared with a likelihood ratio test with a df of 1 using the function *lrtest* (R package *lmtest*; Zeileis & Hothorn, 2002). All scripts were written in R v4.1.3 (R Core Team, 2022).

12

Results

Tree height and rust vulnerability both exhibited high heritabilities (0.469 and 0.666, respectively), high predictive abilities (0.677 and 0.755 respectively), and a strong independence, with an estimated genetic correlation of 0.022. The GWAS did not overfit phenotypic variation: swapping phenotypes (permutation test) among family members of the same block (i.e., only randomly mismatching Mendelian sampling) significantly reduced the average significance of the SNPs ($t_1 < -2.59 \times 10^2$, $p < 0.001$). Only one genetic variant was significantly associated with rust vulnerability, located on chromosome 1, and none for tree height (Fig. 1A, 1B). The Q-Q plot on rust vulnerability revealed that some SNPs were significantly associated with a level of significance well above the 95% confidence interval (Fig. 1D); most of them being in the identified peak. None of the SNPs were significantly associated with tree height after Bayesian shrinkage, and Q-Q plot revealed a classic population structure overcorrection (Fig. 1C).

Common and most heritable alleles structured families

The population under study is structured in a hierarchical way: first into populations, then into families. Population structure, captured by the first eigenvalues (Patterson et al., 2006), substantially shaped genetic diversity, as the first two eigenvalues alone explained more than 50% of the variance (40.0% and 24.5% respectively; Fig. S1). Because the population underwent family selection during breeding in the past, family structure is strong and can even be apprehended visually (Fig. 2). Several statistics significantly supports the strong family structure: (i) randomly shuffling the family ID increased by 9.96 times the within "family" variance ($t_1 = 3.70 \times 10^3$, $p < 0.001$); (ii) when restricting to common alleles, the first two eigenvalues of the PCA still explained a large part of the variance (56.2%), showing that family structure is bound to selection, as expected under family selection.

13

Structure is generally assumed to be reflected by polymorphism at neutral genes scattered across the genome, to the point where samples of SNPs can reveal population structure quite accurately if they are sufficiently large. In order to understand what drove the family structure, similarly to using annotation to focus on some SNPs, we subset 10% of the SNPs first randomly and then according to their MAF, AIM, significance in a GWAS, or additive variance, thus redefining relatedness with a different set of linkage disequilibrium. In our dataset, random samples of SNPs, performed quite poorly compared to the whole set of SNPs ($t_1 = 2.12 \times 10^2$, $p < 0.001$), although the SNPs were scattered along the genome. However, SNPs had a different structuring power at the family level according to the way they were sampled (Fig. 3): SNPs with the largest AIM, performing better than random samples ($t_1 = 3.86 \times 10^2$, $p < 0.001$), and even than the whole set; and SNPs with the largest MAF and the largest additive variance, performing better than random samples ($t_1 > 1.09 \times 10^2$, $p < 0.001$). This result suggests that family structure information is carried by patches over the genome instead of being scattered across the genome.

Local relatedness improves ssGBLUP fit for rust vulnerability

Although the growth of focal individuals was not affected by their neighbors, damage due to rust was more severe the more related the focal individuals were with their neighbors. Indeed, the genomic models incorporating local relatedness as a covariate had significantly higher likelihood than without for rust vulnerability ($\chi^2 = 9.83$, $p = 0.002$), but not for tree height ($\chi^2 = 0.09$, $p = 0.236$). As for family structure which is driven by some SNPs, different categories of SNPs had a different impact on focal phenotypes. When accounting for relatedness via the different subsets of SNPs, the Akaike Information Criterion (AIC) generally decreased (Fig. S2). However, for rust vulnerability, only the subset of SNPs with the largest MAF significantly increased the likelihood of the model ($\chi^2 = 4.02$, $p = 0.04$), that is the one that best captured the family structure. Likelihood was not significantly improved by SNPs with the largest AIM ($\chi^2 = 0.15$, $p = 0.703$) or the largest additive variance ($\chi^2 = 2.65$, $p = 0.104$, respectively), and was significantly worse with other subsets ($\chi^2 > 6.66$, $p <$

0.010). For tree height, no subset of SNPs improved the likelihood ($\chi^2 < 3.48$, $p > 0.062$). In other words, when focal individuals had related individuals in their vicinity, the focal phenotypes were more affected: in this case, the vicinity of related individuals caused significantly more rust damage.

The results suggest that shared vulnerability is the cause of rust damage amplification in the related neighborhood. In support of this claim, the covariance between random pairs of neighboring individuals' rust vulnerability was enriched by local relatedness: from an average of 0.28 for the whole set to 0.43 when only the most related neighbors (highest quartile) were retained, suggesting that local relatedness was a proxy for phenotypic similarity for the trait rather than the cause of plant-to-plant interactions (through kin selection or niche partitioning).

In spite of genomic models being sensitive to local relatedness, improvement of predictive abilities (PA) was limited (Fig. S3) - probably due to a lack of power. Indeed, incorporating local relatedness did not significantly change the PA neither with the whole set of SNPs ($|t_2| < 0.594$, $p > 0.553$), nor with any of the alternative subsets ($|t_2| < 1.03$, $p > 0.301$), with a slightly better PA when incorporating local relatedness for SNPs with the smallest MAF on rust vulnerability ($t_2 = 1.73$, df = 2.00×10^3, $p = 0.0841$), and SNPs with the smallest tree height significance on rust vulnerability ($t_2 = 1.97$, df = 2.00×10^3, $p = 0.0491$). See the Supplementary materials for further details.

15

16

Discussion

Genomic selection in forest tree breeding has successfully predicted growth and wood quality for many species (Lenz et al., 2020), such as Eucalyptus (e.g. Resende et al., 2012), pines (e.g., Isik et al., 2016), or spruces (e.g., Beaulieu et al., 2014). The predictive ability (PA) of the underlying genomic models relies on the ability of genotypic data to capture the covariance between candidate loci, thereby reflecting how much genetic similarity explains phenotypic similarities (Powell et al., 2010). An additional source of phenotypic covariances are micro-environmental effects, and accounting for spatial autocorrelation can enhance genomic predictions (Cappa et al, 2022). In our case, on top of spatial autocorrelation, we accounted for local relatedness, another source of heterogeneity. Results show that part of the plant-to-plant interaction can be ascribed to the relatedness with neighbors. In the case of the Black poplars under study, for rust vulnerability the interaction was more likely due to relatedness being a proxy rather than revealing kin selection/niche partitioning. Additionally, relatedness increases rust damages, whether focal individuals and neighbors are resistant or not, suggesting that inoculum pressure partly increases with relatedness. The lack of diversity at the local scale can hence be detrimental, whatever the level of resistance of individuals.

Differences in genetic architecture driving local relatedness

It is generally assumed that tree height is a complex trait with a highly polygenic architecture, which might not be the case for rust vulnerability (Du et al. 2016; Jorge et al., 2005). The composition of our SNP array may also have had an influence on the way both architectures were '*captured*', as the chip was enriched during its development in QTLs and candidate expression genes related to rust resistance (Faivre-Rampant et al., 2016), but not for height, the most polygenic of the two traits. The low genetic correlation between both traits is consistent with some previous reports (e.g., Beaulieu et al., 2020; Liu et al., 2022), though

17

not all (e.g., Lenz et al., 2021; Cappa et al., 2022); we will assume in our case that orthogonality is strong enough to show that the traits are non-redundant, with independent architectures.

The differences in genetic architecture between the two traits studied, as well as the design of the SNP array, may have determined the results in terms of association, with only one major gene detected (as a peak) for rust, in contrast to the absence of associations for the more polygenic trait. Another element that may have influenced the association for rust is its phenotypic scoring, which is based on a qualitative scale of nine notations. Even if it should be taken cautiously, it is not uncommon to encounter a simpler genetic architecture for response to biotic constraints compared to complex quantitative traits (e.g., gene-for-gene resistance; Flor, 1971; Jorge et al., 2005). Consequently, many haplotype combinations can lead to tall individuals, but few to rust resistance, because a polygenic architecture is redundant; in other words, when individuals are related, their probability of both being resistant is higher than that of both being tall. Local relatedness thus reveals a shared vulnerability within the neighborhood.

Selection of relatedness or co-selection of relatives?

Interactions between neighbors may depend on local relatedness, and whether this interaction is positive or negative depends on the relative strength of kin selection (Hamilton, 1964) and niche partitioning (Silvertown, 2004). As mentioned above, the importance of group selection in nature is still debated, but local relatedness has been shown to be perceived through kin recognition in plant species (e.g., Dudley et al., 2007; Murphy et al., 2009). Such recognition could then lead to favorable (kin selection) or unfavorable (niche partitioning) interactions. One such detrimental interaction is competition. Competition can be accounted for in a quantitative genetic model by assigning to an individual one direct genetic effect (DGE) as the effect of its genes on its own phenotype, and one indirect

18

genetic effect (IGE) as the effect of its genes on phenotypes of surrounding individuals (Griffing, 1967; potential applications in Muir, 2005). Competition occurs when DGE and IGE are negatively correlated. A positive correlation from such a model would suggest a cooperative synergistic interaction. Although adding complexity to the model, including competition has been shown to reduce bias in covariance estimation (Costa e Silva et al., 2013). In our case, in addition to attempts to include interactions, IGE resulted in a lower predictive ability than with the ssGBLUP baseline (results not shown).

The simpler genetic architecture of rust vulnerability compared to that of tree height might play a role in shaping the phenotypes. Family structure was driving similarity of rust vulnerability, and combination of similar vulnerability resulted in increased rust damage. The amplifying effect is even stronger in perennials as shared vulnerability can be perceived by successive generations of pathogens. Consistent with the increased disease resilience conferred by varietal association in a field (e.g., Smithson and Lenne, 1996; Burdon and Thrall, 2009), the local aggregation of susceptible individuals amplified rust damage. Resistance similarity and relatedness were strongly linked, but it is likely that the more complex the genetic architecture, the easier it is to dissociate phenotypic similarity and relatedness.

Once it has been shown that neighbourhood relatedness is indeed correlated with similarity at focal phenotypes, the difficulty in disentangling kin selection from niche partitioning is to determine whether the relatedness is a cause, as an expression of kin selection or niche competition, or a consequence, as an expression of a confounding between relatedness and phenotypic interaction. In the latter case, the focal phenotype would be modified by that of its neighbors through plant-to-plant interactions, and if phenotypic interaction increases when phenotypes are similar (i.e., directional selection, e.g., competition for resource uptake), it can be confused with the effect of relatedness, as genetically related individuals tend to have similar phenotypes.

19

Whether there was kin selection/competition in addition to the phenotypic interaction, or whether we simply lacked statistical power, is difficult to assess. Selection on local relatedness due to kin selection or niche partitioning - selection on relatedness - might be confused with the fact that selection leads to phenotypic convergence, that in turn leads to a genotypic convergence - a co-selection of related. The randomization in the block design and repetition can partly limit this confusion, but it is evident that interpreting the data is fraught with difficulties, as the tallest individuals showed also a higher relatedness with the rest of the population. The fact that family structure was mainly carried by SNPs likely associated with selection (following the hypothesis of Yang et al., 2010 and Biddanda et al., 2020) suggest that relatives were co-selected, as is often the case in breeding programs implementing family selection. An inevitable consequence is that, as seen in crop selection, interesting genotypes for kin selection/cooperation have been lost during domestication (Fréville et al., 2022), making it difficult for genomic selection to account for local relatedness (as predictive abilities show).

20

Acknowledgements

The authors acknowledge the Uppsala University and the European Union's Horizon 2020 B4EST for basic functioning and postdoctoral grant for MT. The authors would like to thank Véronique Jorge and Remy Gobin of the BioForA unit (INRAE, ONF, Orléans, France) for their help in compiling the data. The computations and data handling were enabled by resources provided by the Swedish National Infrastructure for Computing (SNIC 2017-7-296) at UppMax partially funded by the Swedish Research Council through grant agreement no. 2018-05973.

Author Contributions

MT was responsible for writing the report, conducting the search, extracting and analysing data, interpreting results, updating reference lists. LS was responsible for designing the experiments and screening potentially eligible studies. ML and LS contributed to interpreting results and provided feedback on the report.

Competing Interests

The authors declare that there is no conflict of interest.

Data Archiving

The data that support the findings of this study are openly available on DATA INRAE at https://data.inrae.fr/privateurl.xhtml?token=b79ab1ca-ebb9-47c6-9272-1568c0c33d70.

21

Rerefences

Aguilar, I., Legarra, A., Cardoso, F., Masuda, Y., Lourenco, D., & Misztal, I. (2019). Frequentist p-values for large-scale-single step genome-wide association, with an application to birth weight in American Angus cattle. *Genetics Selection Evolution*, *51*(1), 1-8.

Astle, W., & Balding, D. J. (2009). Population structure and cryptic relatedness in genetic association studies. *Statistical Science*, *24*(4), 451-471.

Beaulieu, J., Doerksen, T., Clément, S., MacKay, J., & Bousquet, J. (2014). Accuracy of genomic selection models in a large population of open-pollinated families in white spruce. *Heredity*, *113*(4), 343-352.

Beaulieu, J., Nadeau, S., Ding, C., Celedon, J. M., Azaiez, A., Ritland, C., et al. (2020). Genomic selection for resistance to spruce budworm in white spruce and relationships with growth and wood quality traits. *Evolutionary applications*, *13*(10), 2704-2722.

Biddanda, A., Rice, D. P., & Novembre, J. (2020). A variant-centric perspective on geographic patterns of human allele frequency variation. *Elife*, *9*, e60107.

Bijma, P., & Wade, M. J. (2008). The joint effects of kin, multilevel selection and indirect genetic effects on response to genetic selection. *Journal of evolutionary biology*, *21*(5), 1175-1188.

22

Burdon, J. J., & Thrall, P. H. (2009). Coevolution of plants and their pathogens in natural habitats. *Science*, *324*(5928), 755-756.

Boyle, E. A., Li, Y. I., & Pritchard, J. K. (2017). An expanded view of complex traits: from polygenic to omnigenic. *Cell*, *169*(7), 1177-1186.

Cahill Jr, J. F., & McNickle, G. G. (2011). The behavioral ecology of nutrient foraging by plants. *Annual Review of ecology, evolution, and systematics*, *42*, 289-311.

Calus, M. P., & Veerkamp, R. F. (2011). Accuracy of multi-trait genomic selection using different methods. *Genetics Selection Evolution*, *43*(1), 1-14.

Cappa, E. P., & Cantet, R. J. (2007). Bayesian estimation of a surface to account for a spatial trend using penalized splines in an individual-tree mixed model. *Canadian Journal of Forest Research*, *37*(12), 2677-2688.

Cappa, E. P., de Lima, B. M., da Silva-Junior, O. B., Garcia, C. C., Mansfield, S. D., & Grattapaglia, D. (2019). Improving genomic prediction of growth and wood traits in Eucalyptus using phenotypes from non-genotyped trees by single-step GBLUP. *Plant Science*, *284*, 9-15.

Cappa, E. P., Ratcliffe, B., Chen, C., Thomas, B. R., Liu, Y., Klutsch, J., et al. (2022). Improving lodgepole pine genomic evaluation using spatial correlation structure and SNP selection with single-step GBLUP. *Heredity*, *128*(4), 209-224.

Casper, B. B., & Jackson, R. B. (1997). Plant competition underground. *Annual review of ecology and systematics*, 545-570.

23

Christensen, O. F., & Lund, M. S. 2010. Genomic prediction when some animals are not genotyped. Genetics Selection Evolution 42, 2.

Christensen, O. F., Madsen, P., Nielsen, B., Ostersen, T., & Su, G. (2012). Single-step methods for genomic evaluation in pigs. *animal*, *6*(10), 1565-1571.

Costa e Silva, J., Kerr, R.J. (2013) Accounting for competition in genetic analysis, with particular emphasis on forest genetic trials. *Tree Genetics & Genomes, 9,* 1-17.

Denison, R. F., Kiers, E. T., & West, S. A. (2003). Darwinian agriculture: when can humans find solutions beyond the reach of natural selection? *The quarterly review of biology*, *78*(2), 145-168.

Diouf, I., Derivot, L., Koussevitzky, S., Carretero, Y., Bitton, F., Moreau, L., & Causse, M. (2020). Genetic basis of phenotypic plasticity and genotype× environment interactions in a multi-parental tomato population. Journal of Experimental Botany, 71(18), 5365-5376

Donald, C.M. (1981). Competitive plants, communal plants, and yields in wheat crops. L. Evans, W.J. Peacock (Eds.), Wheat Science – Today and Tomorrow, Cambridge University Press.

Donald, C.M., Hamblin, J. (1983). The convergent evolution of annual seed crops in agriculture. In Advances in agronomy (ed. NC Brady), pp. 97–143. New York, NY: Academic Press.

Dong, L., Xiao, S., Chen, J., Wan, L., & Wang, Z. (2016). Genomic selection using extreme phenotypes and pre-selection of SNPs in large yellow croaker (Larimichthys crocea). *Marine Biotechnology*, *18*(5), 575-583.

Du, Q., Gong, C., Wang, Q., Zhou, D., Yang, H., Pan, W., et al. (2016). Genetic architecture of growth traits in Populus revealed by integrated quantitative trait locus (QTL) analysis and association studies. *New Phytologist*, *209*(3), 1067-1082.

Fisher, R.A. (1918). The correlation between relatives under the supposition of Mendelian inheritance. *Trans. Roy. Soc. Edinburgh 52*, 399-433.

Gualdrón Duarte, J. L., Gori, A. S., Hubin, X., Lourenco, D., Charlier, C., Misztal, I., & Druet, T. (2020). Performances of Adaptive MultiBLUP, Bayesian regressions, and weighted-GBLUP approaches for genomic predictions in Belgian Blue beef cattle. *BMC genomics*, *21*(1), 1-18.

Dudley, S. A., & File, A. L. (2007). Kin recognition in an annual plant. *Biology Letters*, *3*(4), 435-438.

Emik, L. O., & Terrill, C. E. (1949). Systematic procedures for calculating inbreeding coefficients. *Journal of Heredity*, *40*(2), 51-55.

Faivre-Rampant, P., Zaina, G., Jorge, V., Giacomello, S., Segura, V., Scalabrin, S., et al. (2016). New resources for genetic studies in Populus nigra: Genome-wide SNP discovery and development of a 12k Infinium array. *Molecular ecology resources*, *16*(4), 1023-1036.

Falconer, D.S. (1989). Introduction to quantitative genetics (3rd edition, p. 129). Pearson Education India.

Feau, N., Joly, D. L., & Hamelin, R. C. (2007). Poplar leaf rusts: model pathogens for a model tree. *Botany*, *85*(12), 1127-1135.

25

File, A. L., Murphy, G. P., & Dudley, S. A. (2012). Fitness consequences of plants growing with siblings: reconciling kin selection, niche partitioning and competitive ability. *Proceedings of the Royal Society B: Biological Sciences*, *279*(1727), 209-218.

Flor, H. H. (1971). Current status of the gene-for-gene concept. *Annual review of phytopathology*, *9*(1), 275-296.

Fréville, H., Montazeaud, G., Forst, E., David, J., Papa, R., & Tenaillon, M. I. (2022). Shift in beneficial interactions during crop evolution. *Evolutionary Applications*, *15*(6), 905-918.

Garcia-Baccino, C. A., Legarra, A., Christensen, O. F., Misztal, I., Pocrnic, I., Vitezica, Z. G., & Cantet, R. J. (2017). Metafounders are related to F st fixation indices and reduce bias in single-step genomic evaluations. *Genetics Selection Evolution*, *49*(1), 1-14.

Goldsmith, J., Scheipl, F., Huang, L., Wrobel, J., Di, C., Gellar, J., et al. (2022). refund: Regression with Functional Data. R package version 0.1-26. https://CRAN.R-project.org/package=refund

Griffing, B. (1967). Selection in reference to biological groups I. Individual and group selection applied to populations of unordered groups. *Australian Journal of Biological Sciences*, *20*(1), 127-140.

Hamilton, W. D. (1964). The genetical evolution of social behaviour. II. *Journal of theoretical biology*, *7*(1), 17-52.

Isik, F., Bartholomé, J., Farjat, A., Chancerel, E., Raffin, A., Sanchez, L., et al. (2016). Genomic selection in maritime pine. *Plant Science*, *242*, 108-119.

Jorge, V., Dowkiw, A., Faivre-Rampant, P., & Bastien, C. (2005). Genetic architecture of qualitative and quantitative *Melampsora larici-populina* leaf rust resistance in hybrid poplar: genetic mapping and QTL detection. *New Phytologist*, *167*(1), 113-127.

Kijas, J., Elliot, N., Kube, P., Evans, B., Botwright, N., King, H., et al. (2017). Diversity and linkage disequilibrium in farmed Tasmanian Atlantic salmon. *Animal genetics*, *48*(2), 237-241.

Legarra, A., Aguilar, I., & Misztal, I. (2009). A relationship matrix including full pedigree and genomic information. *Journal of dairy science*, *92*(9), 4656-4663.

Legarra, A., Christensen, O. F., Vitezica, Z. G., Aguilar, I., & Misztal, I. (2015). Ancestral relationships using metafounders: finite ancestral populations and across population relationships. *Genetics*, *200*(2), 455-468.

Legionnet, A., Muranty, H., & Lefèvre, F. (1999). Genetic variation of the riparian pioneer tree species Populus nigra. II. Variation in susceptibility to the foliar rust Melampsora larici-populina. *Heredity*, *82*(3), 318-327.

Lenz, P. R., Nadeau, S., Mottet, M. J., Perron, M., Isabel, N., Beaulieu, J., & Bousquet, J. (2020). Multi-trait genomic selection for weevil resistance, growth, and wood quality in Norway spruce. *Evolutionary applications*, *13*(1), 76-94.

Lesaffre, T., & Billiard, S. (2021). On Deleterious Mutations in Perennials: Inbreeding Depression, Mutation Load, and Life-History Evolution. *The American Naturalist*, *197*(5), E143-E155.

27

Lewontin, R. C. (1970). The units of selection. *Annual review of ecology and systematics*, 1-18.

Li, B., Zhang, N., Wang, Y. G., George, A. W., Reverter, A., & Li, Y. (2018). Genomic prediction of breeding values using a subset of SNPs identified by three machine learning methods. *Frontiers in genetics*, *9*, 237.

Liu, Y., Erbilgin, N., Ratcliffe, B., Klutsch, J. G., Wei, X., Ullah, A., et al. (2022). Pest defences under weak selection exert a limited influence on the evolution of height growth and drought avoidance in marginal pine populations. *Proceedings of the Royal Society B*, *289*(1982), 20221034.

Lu, S., Liu, Y., Yu, X., Li, Y., Yang, Y., Wei, M., et al. (2020). Prediction of genomic breeding values based on pre-selected SNPs using ssGBLUP, WssGBLUP and BayesB for Edwardsiellosis resistance in Japanese flounder. *Genetics Selection Evolution*, *52*(1), 1-10.

Luo, Z., Yu, Y., Xiang, J., & Li, F. (2021). Genomic selection using a subset of SNPs identified by genome-wide association analysis for disease resistance traits in aquaculture species. *Aquaculture*, *539*, 736620.

Maynard Smith, J. (1964). Group selection and kin selection. *Nature*, *201*(4924), 1145-1147.

Meuwissen, T. H. E. (1997). Maximizing the response of selection with a predefined rate of inbreeding. *Journal of animal science*, *75*(4), 934-940.

Meuwissen, T. H., Hayes, B. J., & Goddard, M. (2001). Prediction of total genetic value using genome-wide dense marker maps. *genetics*, *157*(4), 1819-1829.

28

Milbau, A., Reheul, D., De Cauwer, B., & Nijs, I. (2007). Factors determining plant–neighbour interactions on different spatial scales in young species-rich grassland communities. *Ecological research*, *22*(2), 242-247.

Miller, D. L. (2022). porridge: Principal Co-Ordinate Ridge Regression. R package version 1.2.

Montazeaud, G., Rousset, F., Fort, F., Violle, C., Fréville, H., & Gandon, S. (2020). Farming plant cooperation in crops. *Proceedings of the Royal Society B*, *287*(1919), 20191290.

Muir, W. M. (2005). Incorporation of competitive effects in forest tree or animal breeding programs. *Genetics*, *170*(3), 1247-1259.

Muñoz, F., and Sanchez, L. (2020). breedR: Statistical Methods for Forest Genetic Resources Analysts. R package version 0.12-5. https://github.com/famuvie/breedR

Murphy, G. P., & Dudley, S. A. (2009). Kin recognition: competition and cooperation in Impatiens (Balsaminaceae). *American journal of botany*, *96*(11), 1990-1996.

Murphy, G. P., Swanton, C. J., Van Acker, R. C., & Dudley, S. A. (2017). Kin recognition, multilevel selection and altruism in crop sustainability. *Journal of Ecology (Oxford)*, *105*(4), 930-934.

Okasha, S. (2020). Altruism, group selection and correlated interaction. *The British journal for the philosophy of science*.

Patterson, N., Price, A. L., & Reich, D. (2006). Population structure and eigenanalysis. *PLoS genetics*, *2*(12), e190.

Pégard, M., Rogier, O., Bérard, A., Faivre-Rampant, P., Paslier, M. C. L., Bastien, C., et al. (2019). Sequence imputation from low density single nucleotide polymorphism panel in a black poplar breeding population. *BMC genomics*, *20*(1), 1-16.

Pégard, M., Segura, V., Muñoz, F., Bastien, C., Jorge, V., & Sanchez, L. (2020). Favorable conditions for genomic evaluation to outperform classical pedigree evaluation highlighted by a proof-of-concept study in poplar. *Frontiers in plant science*, *11*, 581954.

Powell, J. E., Visscher, P. M., & Goddard, M. E. (2010). Reconciling the analysis of IBD and IBS in complex trait studies. *Nature Reviews Genetics*, *11*(11), 800-805.

R Core Team (2022). R: A language and environment for statistical computing. R Foundation for Statistical Computing, Vienna, Austria. URL. https://www.R-project.org/

Ratcliffe, B., El-Dien, O. G., Cappa, E. P., Porth, I., Klápště, J., Chen, C., & El-Kassaby, Y. A. (2017). Single-step BLUP with varying genotyping effort in open-pollinated Picea glauca. *G3: Genes, Genomes, Genetics*, *7*(3), 935-942.

Resende, M. D., Resende Jr, M. F., Sansaloni, C. P., Petroli, C. D., Missiaggia, A. A., Aguiar, A. M., et al. (2012). Genomic selection for growth and wood quality in Eucalyptus: capturing the missing heritability and accelerating breeding for complex traits in forest trees. *New Phytologist*, *194*(1), 116-128.

Rosenberg, N. A., Li, L. M., Ward, R., & Pritchard, J. K. (2003). Informativeness of genetic markers for inference of ancestry. *The American Journal of Human Genetics*, *73*(6), 1402-1422.

30

Sanchez, M. P., Govignon-Gion, A., Croiseau, P., Fritz, S., Hozé, C., Miranda, G., et al. (2017). Within-breed and multi-breed GWAS on imputed whole-genome sequence variants reveal candidate mutations affecting milk protein composition in dairy cattle. *Genetics Selection Evolution*, *49*(1), 1-16.

Silvertown, J. (2004). Plant coexistence and the niche. *Trends in Ecology & evolution*, *19*(11), 605-611.

Smithson, J. B., & Lenne, J. M. (1996). Varietal mixtures: a viable strategy for sustainable productivity in subsistence agriculture. *Annals of applied biology*, *128*(1), 127-158.

Stephens, M. (2017). False discovery rates: a new deal. *Biostatistics*, *18*(2), 275-294.

Thistlethwaite, F. R., Gamal El-Dien, O., Ratcliffe, B., Klápště, J., Porth, I., Chen, C., et al. (2020). Linkage disequilibrium vs. pedigree: Genomic selection prediction accuracy in conifer species. *PLoS One*, *15*(6), e0232201.

Tiret, M., & Milesi, P. Statistical Peak Detection for GWAS. Zenodo. https://doi.org/10.5281/zenodo.5079556. Deposited 7 July 2021.

Tsai, H. Y., Matika, O., Edwards, S. M., Antolín–Sánchez, R., Hamilton, A., Guy, D. R., et al. (2017). Genotype imputation to improve the cost-efficiency of genomic selection in farmed Atlantic salmon. *G3: Genes, genomes, genetics*, *7*(4), 1377-1383.

VanRaden, P. M. (2008). Efficient methods to compute genomic predictions. *Journal of dairy science*, *91*(11), 4414-4423.

31

Weiner, J., Andersen, S. B., Wille, W. K. M., Griepentrog, H. W., & Olsen, J. M. (2010). Evolutionary Agroecology: the potential for cooperative, high density, weed-suppressing cereals. *Evolutionary Applications*, *3*(5-6), 473-479.

Weiner, J., Du, Y. L., Zhang, C., Qin, X. L., & Li, F. M. (2017). Evolutionary agroecology: individual fitness and population yield in wheat (Triticum aestivum).

Weiner, J. (2019). Looking in the wrong direction for higher-yielding crop genotypes. *Trends in Plant Science*, *24*(10), 927-933.

Wilson, D. S., & Wilson, E. O. (2007). Rethinking the theoretical foundation of sociobiology. *The Quarterly review of biology*, *82*(4), 327-348.

Yang, J., Benyamin, B., McEvoy, B. P., Gordon, S., Henders, A. K., Nyholt, D. R., et al. (2010). Common SNPs explain a large proportion of the heritability for human height. *Nature genetics*, *42*(7), 565-569.

Zeileis, A., & Hothorn, T. (2002). Diagnostic Checking in Regression Relationships. R News 2(3), 7-10.

Zhang, Z., Liu, J., Ding, X., Bijma, P., de Koning, D. J., & Zhang, Q. (2010). Best linear unbiased prediction of genomic breeding values using a trait-specific marker-derived relationship matrix. *PloS one*, *5*(9), e12648.

32

Figures

Figure 1. GWAS on tree height and rust vulnerability in Populus nigra. **(A)**. Manhattan plot of the GWAS on tree height. The dots are the log significance of the markers. The solid horizontal line stands for the 5% significance level, and the dashed horizontal line stands for the 5% FDR level. The vertical dashed lines are position where significant hits were detected as being part of a peak. **(B)**. Idem as panel A, for rust vulnerability. **(C)**. Q-Q plot of the GWAS on tree height. The dots were the quantile of the markers; the solid line is the 1-slope segment; the gray cross is the position of the median; and the gray area is the 95% confidence interval. **(D)**. Idem as panel C, for rust vulnerability.

Figure 2. The first two axes of the Multidimensional Scaling (MDS) of Populus nigra. **(A)**. MDS with labels of the fathers (with black large shapes). Colored and smaller shapes are the offspring, the shape corresponding to its father. **(B)**. The same MDS as in panel A., but labeled for the mothers.

Figure 3. Within family variance (V_F) for each subset of SNPs. The black dashed horizontal line is the average V_F of randomly sampled SNPs, the gray dashed horizontal lines delimit the 95% confidence interval, and the black horizontal dotted line is V_F of the entire set of SNPs. Red dots are when selected for tree height, and blue for rust vulnerability. SNP subsets: largest or smallest MAF (+ or - MAF), largest or smallest AIM (+ or - AIM), most or least significant (+ or - $\log_{10}(p)$), and most or least heritable for tree height (+ or - h^2).

33

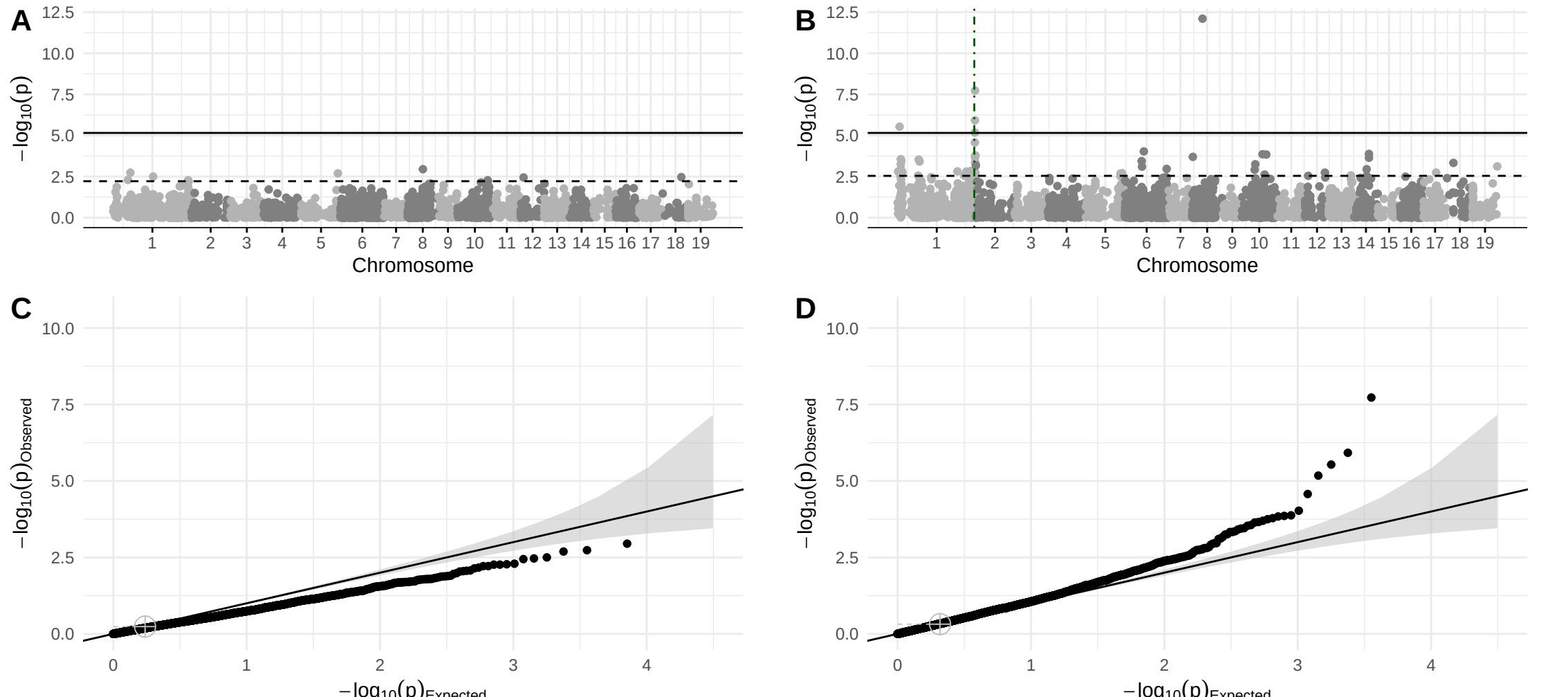
A
B
C
D
$-\log_{10}(p)$
Chromosome
$-\log_{10}(p)_{Observed}$
$-\log_{10}(p)_{Expected}$

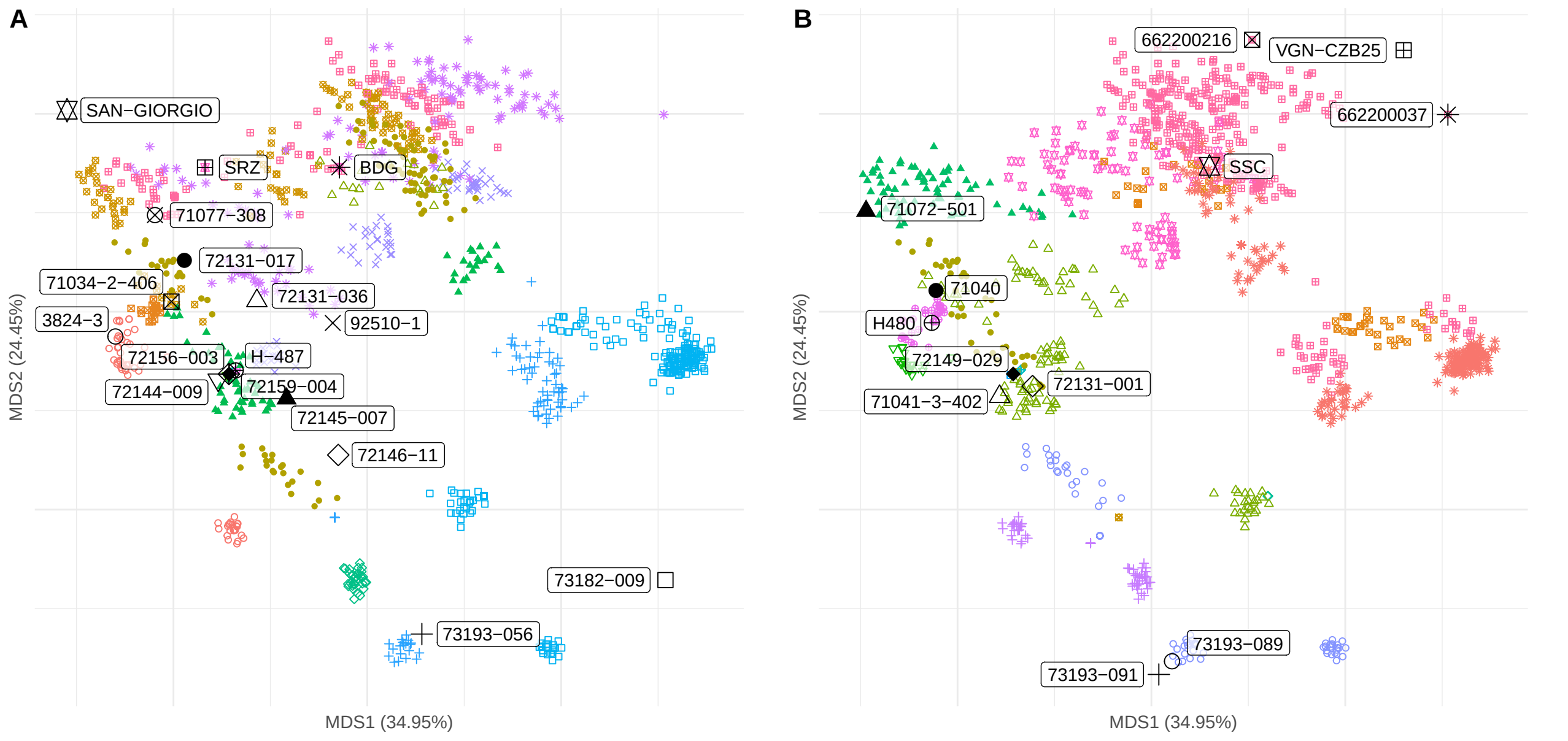
A
SAN−GIORGIO
SRZ
BDG
71077−308
72131−017
71034−2−406
72131−036
3824−3
92510−1
72156−003
H−487
72144−009
72159−004
72145−007
72146−11
73182−009
73193−056
MDS2 (24.45%)
MDS1 (34.95%)
B
662200216
VGN−CZB25
662200037
SSC
71072−501
71040
H480
72149−029
72131−001
71041−3−402
73193−089
73193−091
MDS2 (24.45%)
MDS1 (34.95%)

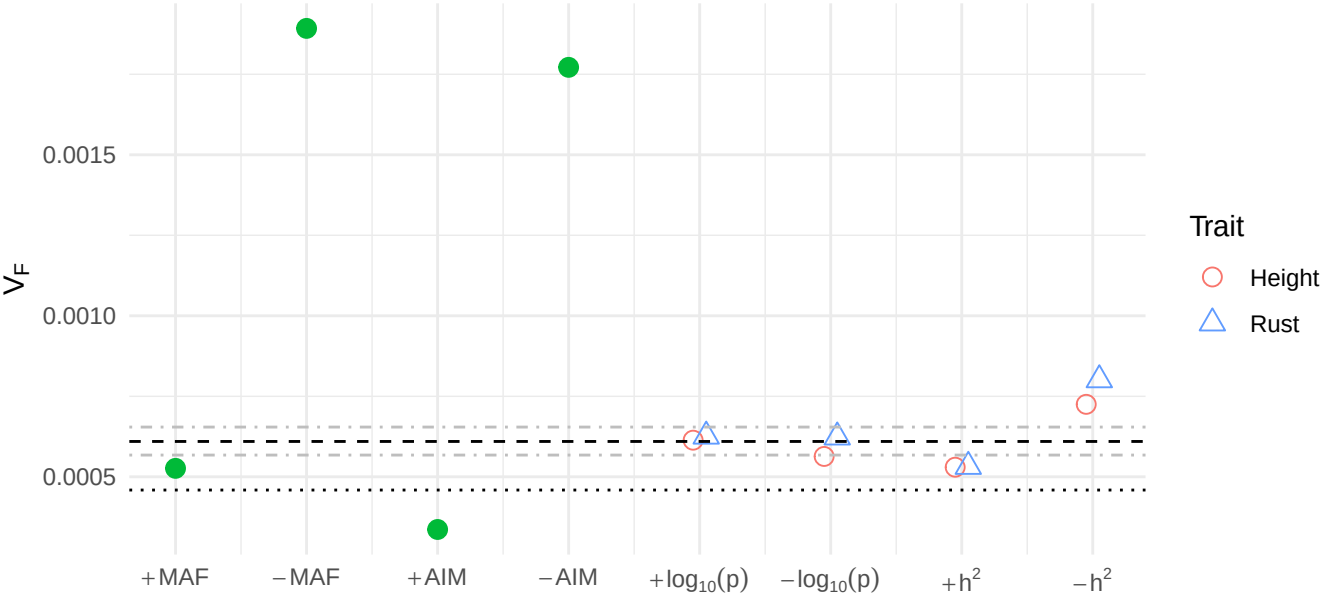
V_F
0.0015
0.0010
0.0005
+MAF
−MAF
+AIM
−AIM
+log10(p)
−log10(p)
+h2
−h2
Trait
Height
Rust